17th World Conference on Earthquake Engineering, 17WCEE
Sendai, Japan - September 13th to 18th 2020

STUDY ON VERTICAL MECHANICAL PROPERTIES AND PARAMETER CORRELATION OF ROTATING 3D ISOLATION BEARINGS

S. F. Wu[1], W. G. Liu[2], Q. Zhang[3], Z. K. Ding[4]

[1] *PhD candidate, Shanghai University, shanghai200444, China, BWCX_WSF@163.com.*

[2] *Professor, Shanghai University, shanghai200444, China, liuwg@aliyun.com.*

[3] *Master, Shanghai University, shanghai200444, China, 119226734@qq.com.*

[4] *Shanghai Nuclear Engineering Research and Design Institute, Shanghai, 200233, China, dingzk@snerdi.com.*

Abstract

Conventional isolation devices can reduce the structural response in horizontal directions only, but it does not reduce the structural response in vertical directions. However, the vertical earthquake motions may be severely distinct, even higher than horizontal component, and strong vertical ground motions and structural damage have been observed across the world. Then, vertical earthquakes are usually underestimated. In this paper, an innovative rotating three-dimensional (3D) seismic isolator were described, which were assembled using three inclined lead rubber bearing (LRB), one horizontal LRB and a rotating steel block. The vertical displacement transforms into compression-shear deformation of the inclined lead rubber bearings (LRBs) and frictional rotating of the friction block. It has large bearing capacity and low vertical stiffness due to oblique shear deformation of inclined LRBs. The shear, compression and torsion of mechanical properties of vertical isolation bearings are studied. A new kind of non-parallel hysteretic model of vertical stiffness was illustrated. The difference between proposed model and conventional bilinear model is that the load stiffness is larger than unload stiffness. Besides, theoretical equation considered on friction force of vertical stiffness was conducted. Vertical compression test of model device was conducted. It can be concluded from the test results that the device has bilinear behavior and plump hysteretic loop in vertical direction. Vertical properties remain stable with variable loading. The theoretical value and test of vertical stiffness are similar, whose errors are within 15%. The proposed hysteretic model can efficiently simulate the vertical mechanical behavior of a 3D seismic isolation system. The effects of different parameters are highlighted based on the theoretical mechanical model. The friction coefficient and inclination angle of the inclined LRBs strongly influence the vertical behavior of the proposed device. When the friction coefficient is 0, the loading and unloading stiffness remain the same, and the mechanical model degenerates into a conventional bilinear model. When friction exists, the loading stiffness is greater. The maximum vertical load is defined as the vertical load when the shear strain of the inclined LRB is 300%. The maximum vertical load and vertical yielding load decrease with increasing inclination angle and decreasing friction coefficient. The influence of the friction for the vertical load of device reduces with increasing inclination angles. In summary, the 3D seismic isolator has good vertical mechanical properties, which can provide reference value for the practical engineering design and application of the novel rotating 3D seismic isolator.

Keywords: three-dimensional isolation; lead rubber bearing; vertical performance; compression test; bearing parameters

1. Introduction

Seismic isolation is a method to reduce damage to the superstructure during earthquake ground motions. It are reduced by lengthening the fundamental period of vibration and added damping through the introduction of isolators with low horizontal and large vertical stiffness that decouple the superstructure from the supporting substructure. Observations of the response of numerous base-isolated buildings in past earthquakes, mostly favorable, have been reported. Although problems with expansion joints and some disruption of contents have been observed, significant nonstructural component damage has not been reported. (Staehlin et al. 1996; Gavin and Nigbor 2012; Ryan et al. 2016). It has been proved an efficient method to protect structures from earthquake damage (Architectural Society of Japan, 2006). But conventional isolation devices can reduce the structural response in horizontal directions only. And it does not reduce the structural response in vertical directions. The vertical earthquake motions may be severely distinct, even higher than horizontal component. Besides, strong vertical ground motions and structural damage have been observed across the world (Yang and Lee, 2007). While vertical earthquakes are usually underestimated, seismic isolation needs to balance the relationship of the low stiffness and support upper structure to realize vertical isolation.

A new 3D isolation system was put forward (Fujita et al, 1996), using disc springs as vertical isolators and rubber bearings as horizontal isolators. The retrofitting of the Pestalozzi school in Yugoslavia using thick rubber bearings is the first application of 3D isolation system (Garevski et al, 2000). A device using metal bellows in the vertical direction and rubber bearing in the horizontal direction was proposed (Ogiso et al. 2003). Development of 3D seismic isolation technology for the next generation of nuclear power plants (NPPs) in Japan was introduced (Masaki et al. 2003) and (Inoue et al. 2004). A nonlinear spring mechanism consisting of an A-shaped link, coil springs, and a linear guide was proposed (Ueda et al. 2007). A 3D isolation device was composed of a horizontal rubber bearing, vertical air spring, and sliders, which was installed in a three story reinforced concreted apartment building in Tokyo (Tomizawa et al. 2012). The mechanics performance test and seismic behavior of a novel 3D isolation bearing for bridges were discussed (Jia et al. 2013). The model of the 3D rotational seismic isolation device was designed, and its vertical compression tests were performed (Liu et al. 2013). Research on distributed flexibility and damping strategy was conducted (Vu et al. 2014). The properties of existing 3D isolation systems and their potential applications to modern nuclear facilities were discussed (Zhou et al. 2016). The fundamental dynamic response of structures with 3D isolation systems is explored, and target horizontal and vertical spectra for a representative strong motion site were developed (Eltahawy. 2017). Static test and seismic dynamic response of an innovative 3D seismic isolation system were discussed (Liu et al. 2018). Additionally, persistent and intensive research on 3D isolation is still needed.

This paper focused on an innovative rotating 3D seismic isolator, which was assembled using three inclined LRBs. The vertical displacement transforms into compression-shear deformation of the inclined LRBs and rotating friction block. It has large bearing capacity and low vertical stiffness due to shear-torque-compression deformation of inclined LRBs. The non-parallel hysteretic model of vertical isolation bearings was illustrated. Besides, vertical compression test and parametric analysis of model device was conducted.

2. Vertical mechanical properties and static test of the 3D isolation bearing

2.1 Composition of 3D isolation device

An innovation 3D oblique rotating friction seismic isolator (3D ORFSI) is introduced in which bearing are installed with inclination. Proposed device consists of horizontal rubber bearing, rotating block, friction blocks, connection blocks, inclined bearings and steel tubes. The sketch and deformation of 3D seismic isolation device is shown in Fig.1. The inclined LRBs are installed symmetrically in a circle. The vertical displacement transforms into compression-shear-torsion deformation of the inclined LRBs and frictional rotating of the friction blocks, and the rotating steel block is rotating.

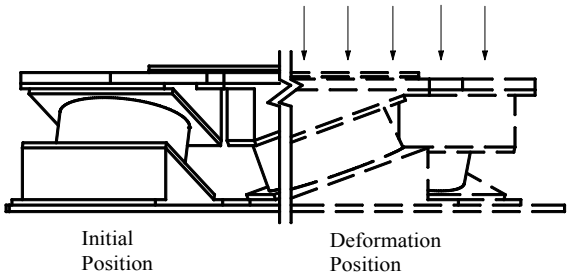

Fig. 1 Sketch and deformation of 3D seismic isolation device

2.2 Mechanical model

Vertical loop is asymmetric quadrangle. Differ from conventional bilinear hysteretic model, the stiffness in load process and unload process are different. Mechanical Model of 3D ORFSI is established based on test results, as is displayed in Fig.2.

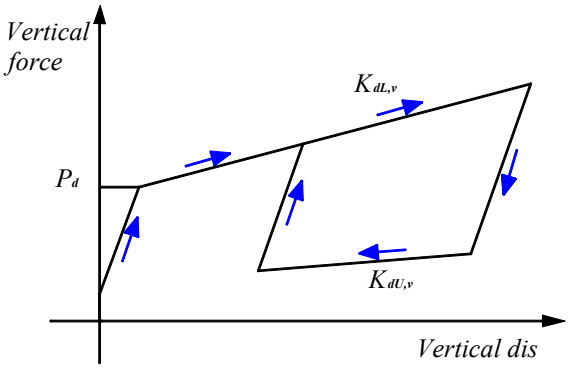

Fig. 2 Non-parallel oblique hysteretic model of 3D seismic isolation device

In this paper, the vertical compressive behavior of the 3D ORFSI is mainly investigated. The 3D ORFSI is a system that consists of a horizontal rubber bearing and three inclined LRBs. The contribution of the horizontal rubber bearing on the vertical stiffness is ignored because its vertical stiffness is much greater. The mechanical analysis of inclined LRB under vertical load is shown in Fig. 3.

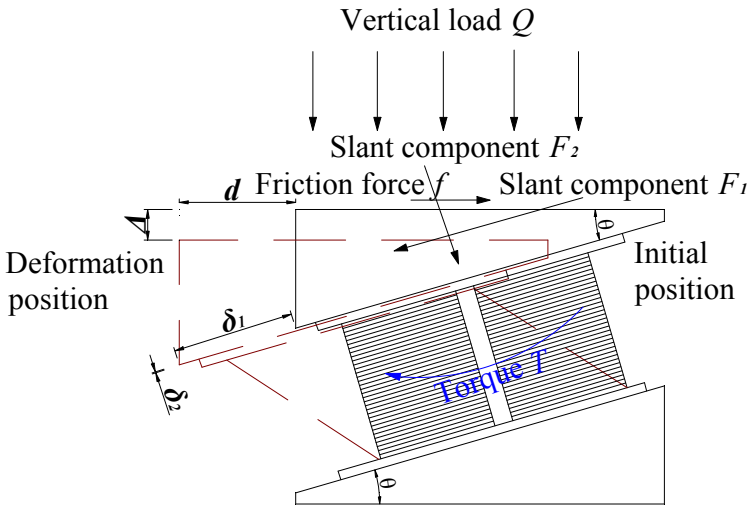

Fig. 3 Mchanical analysis of the inclined LRBs

The radius and width of concentric circles are r and dr on the rotating steel blocks, respectively. The moment of friction is considered by the following formula.

$$dM = -\mu \frac{Q}{\pi R^2} 2\pi r dr \cdot r = \frac{-2\mu r^2 Q}{R^2} dr \tag{1}$$

The negative sign means the resistance moment of friction. The radial-integral of the above formula can obtain the moment of friction, as showing in the formula.

$$M_f = \int dM = \int_0^R \frac{2\mu r^2 Q}{R^2} dr = \frac{2}{3} \mu Q R \tag{2}$$

The friction component of a single bearing is

$$f = \frac{M_f}{3\mathrm{r}} = \frac{2}{9} \mu Q \frac{R}{r} \tag{3}$$

For a lead rubber bearing, the torsional stiffness can be expressed as:

$$K_\varphi = \frac{\pi G r^4}{32 T_r} \tag{4}$$

The relationship between the vertical displacement of the device and the torsional angle of the inclined bearing is as follows:

$$\phi \cdot R \cdot \tan\theta = \Delta_v \tag{5}$$

Torsional stiffness of 3D inclined bearing is

$$K_\phi = n K_d R^2 + \frac{n\pi G r^4}{32 T_r} \tag{6}$$

The torque of a single bearing is:

$$T = \frac{K_\phi \cdot \phi}{r} \tag{7}$$

According to the deformation of the vertical inclined bearings in Fig. 3, the force analysis shows that:

$$\begin{cases} Q\sin\theta - f\cos\theta - T\cos\theta - F_1 = 0 \\ Q\cos\theta + f\sin\theta + T\cos\theta - F_2 = 0 \end{cases} \tag{8}$$

$$F_1 = \delta_1 K_d \quad ; \quad F_2 = \delta_2 K_V \tag{9}$$

$$\Delta_V = \delta_1 \sin\theta + \delta_2 \cos\theta \tag{10}$$

The vertical post-yield stiffness is

$$K_{\mathrm{vd,L}} = \frac{n \cdot \mathrm{d}Q}{\mathrm{d}\Delta_V} = \frac{n K_d K_v}{K_v(\sin^2\theta - \frac{2}{9}\mu\frac{R}{r}\sin\theta\cos\theta - \frac{K_\varphi \sin\theta\cos\theta}{Rr\tan\theta \cdot K_{vd,L}}) + K_d(\cos^2\theta + \frac{2}{9}\mu\frac{R}{r}\sin\theta\cos\theta + \frac{K_\varphi \sin\theta\cos\theta}{Rr\tan\theta \cdot K_{vd,L}})} \tag{11}$$

Simplified, the vertical post-yield stiffness of the 3D ORFSI is obtained as follows:

$$K_{vd,L}=\frac{nK_dK_v+n\dfrac{(K_v-K_d)K_\phi\cos^2\theta}{Rr}}{K_v(\sin^2\theta-\dfrac{2}{9}\mu\dfrac{R}{r}\sin\theta\cos\theta)+K_d(\cos^2\theta+\dfrac{2}{9}\mu\dfrac{R}{r}\sin\theta\cos\theta)} \tag{12}$$

The vertical post-yield loading of the 3D ORFSI is

$$Q_{d,v}=\frac{nQ_d}{sin\theta\ -\ \dfrac{2}{9}\mu\dfrac{R}{r}cos\theta} \tag{13}$$

Where M_f = rotating moment of the rotating steel block; n = number of the inclined LRBs; θ = inclination angle of the connection block; R and r = radius of the rotating steel block and the inclined bearing, respectively; μ = friction coefficient of the friction block and the horizontal rubber bearing; ϕ is torsion angle; $K\phi$ = torque of the rubber bearing; $K\varphi$ = torsional stiffness of the laminated rubber bearing; T = torque of a rubber bearing; Δ_v = vertical displacement of 3D inclined bearing.

The vertical post-yield stiffness of 3D ORFSI in unload process can be obtained with the same method, which is:

$$K_{vd,U}=\frac{nK_dK_v+n\dfrac{(K_v-K_d)K_\phi\cos^2\theta}{Rr}}{K_v(\sin^2\theta+\dfrac{2}{9}\mu\dfrac{R}{r}\sin\theta\cos\theta)+K_d(\cos^2\theta-\dfrac{2}{9}\mu\dfrac{R}{r}\sin\theta\cos\theta)} \tag{14}$$

2.3 Static test

A vertical compression test of a model device was conducted. The load equipment was a hydraulic servo press machine. The maximum vertical load was 2000t, and maximum horizontal load was 400t. A loading equipment is shown in Fig.4.

Fig. 4 Loading equipment

In order to study the vertical mechanical properties of the 3D ORFSI, the effects of inclination angle on vertical stiffness and hysteretic behavior are discussed. Cases1~2 was the angle of 15°of bearing. The vertical force of cases1~2 were 300~800 and 500~1000kN, respectively. Cases3~5 was the angle of 25°of bearing. The vertical force of cases3~5 were 250~550, 350~700 and 300~900kN, respectively. The real

graph of 3D seismic isolation device is shown in Fig. 5. Mechanical parameters of used LRBs inTable 1. Test curves are shown in Fig. 6.

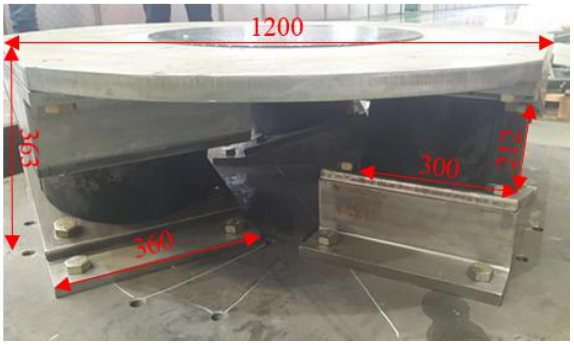

Fig. 5 Real graph of 3D seismic isolation device

Table 1 Mechanical parameters of LRB300

Parameter	Value
Diameter (mm)	300
Total rubber thickness (mm)	60
First shape factor S1	30
Second shape factor S2	5
Vertical stiffness, *Kv* (kN/mm)	1209
Post-yield stiffness, *Kd* (kN/mm)	0.668

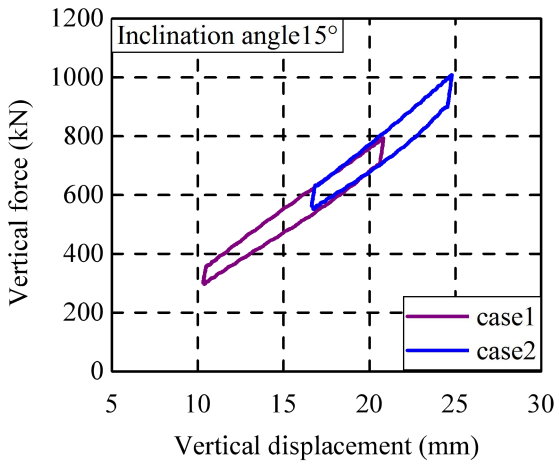

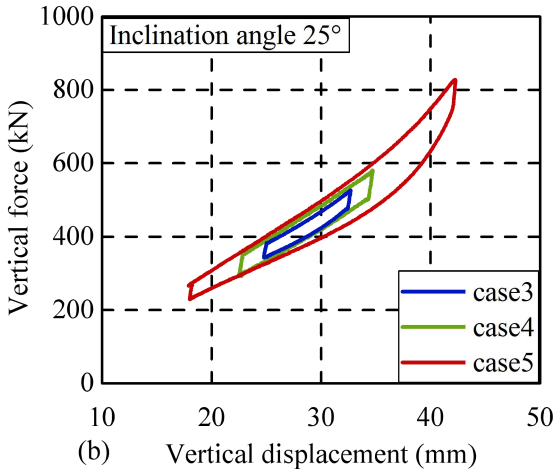

(b)

Fig. 6 Hysteretic curve of the different cases: (a) Cases1~2 was the angle of 15°of bearing. The vertical force of cases1~2 were 300~800 and 500~1000kN, respectively. (b) Cases3~5 was the angle of 25°of bearing. The vertical force of cases3~5 were 250~550, 350~700 and 300~900kN, respectively.

Test value and theory value are approximate and errors are within 15%. Theory value and test results is list in Table 2. Comparison of theory loop and test loops is shown in Fig. 7. The loops match well. Presented mechanical model can simulate vertical behavior of 3D ORFSI efficiently.

Table 2 Vertical stiffness of 3D isolator

Case	Vertical stiffness $K_{vd,L}$(kN/mm)		
	Test	Theory	Error
Case1	35	40	14.29%
Case2	38	40	5.26%
Case3	15	14	6.67%
Case4	13	14	7.69%
Case5	16	14	12.50%

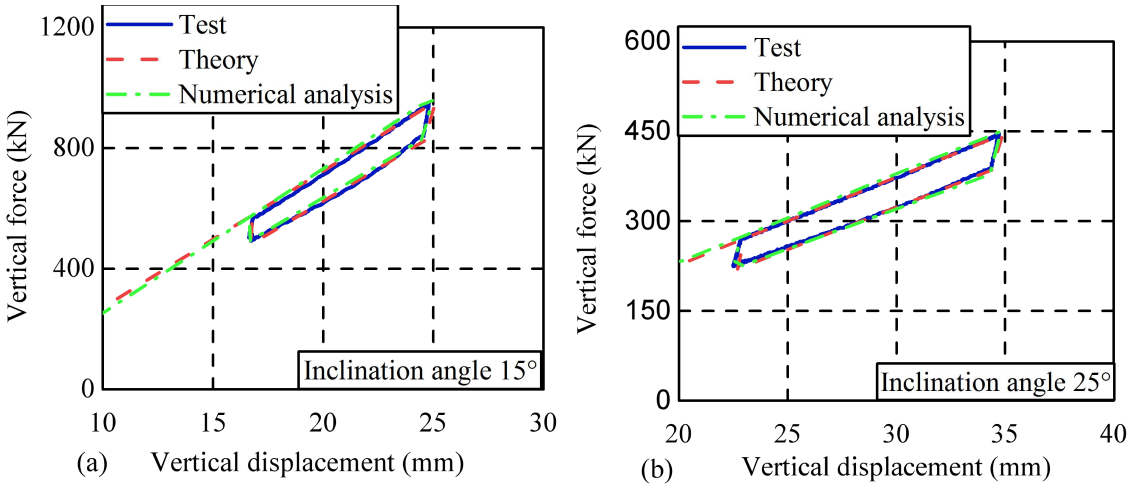

Fig. 7 Comparison of theory and test: (a) Comparison of test loop, theory loop and numerical analysis loop of inclination angle 15° for case 2; (b) Comparison of test loop, theory loop and numerical analysis loop of inclination angle 25° for case 4.

3. Parametric analysis of the mechanical properties of 3D ORFSI

In order to further study the vertical mechanical properties of the 3D ORFSI, the inclination angle and friction coefficient parameters are analyzed. The variation in the mechanical properties with different parameter values can be obtained according to proposed theoretical model in the previous section. The

calculation model is based on a device in which three LRB300s are used as the inclined LRBs. The geometry and mechanical properties of the selected LRB300s are shown in Table 3.

Table 3 Mechanical parameters of LRB300

Parameter	Value
Diameter(mm)	300
Total rubber thickness (mm)	60
Lead core diameter (mm)	70
Shear modulus (MPa)	0.6
First shape factor S1	30
Second shape factor S2	5
Vertical stiffness, Kv (kN/mm)	1209
Post-yield stiffness, Kd (kN/mm)	0.668

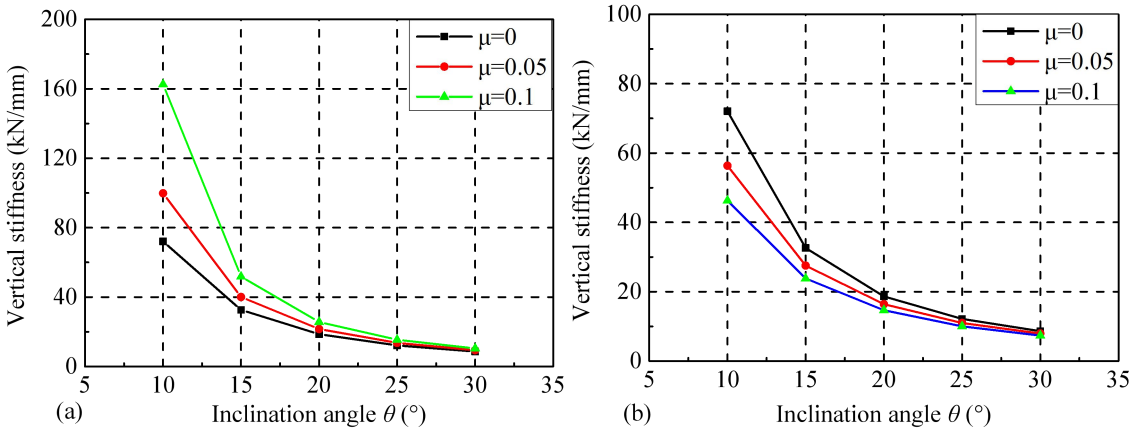

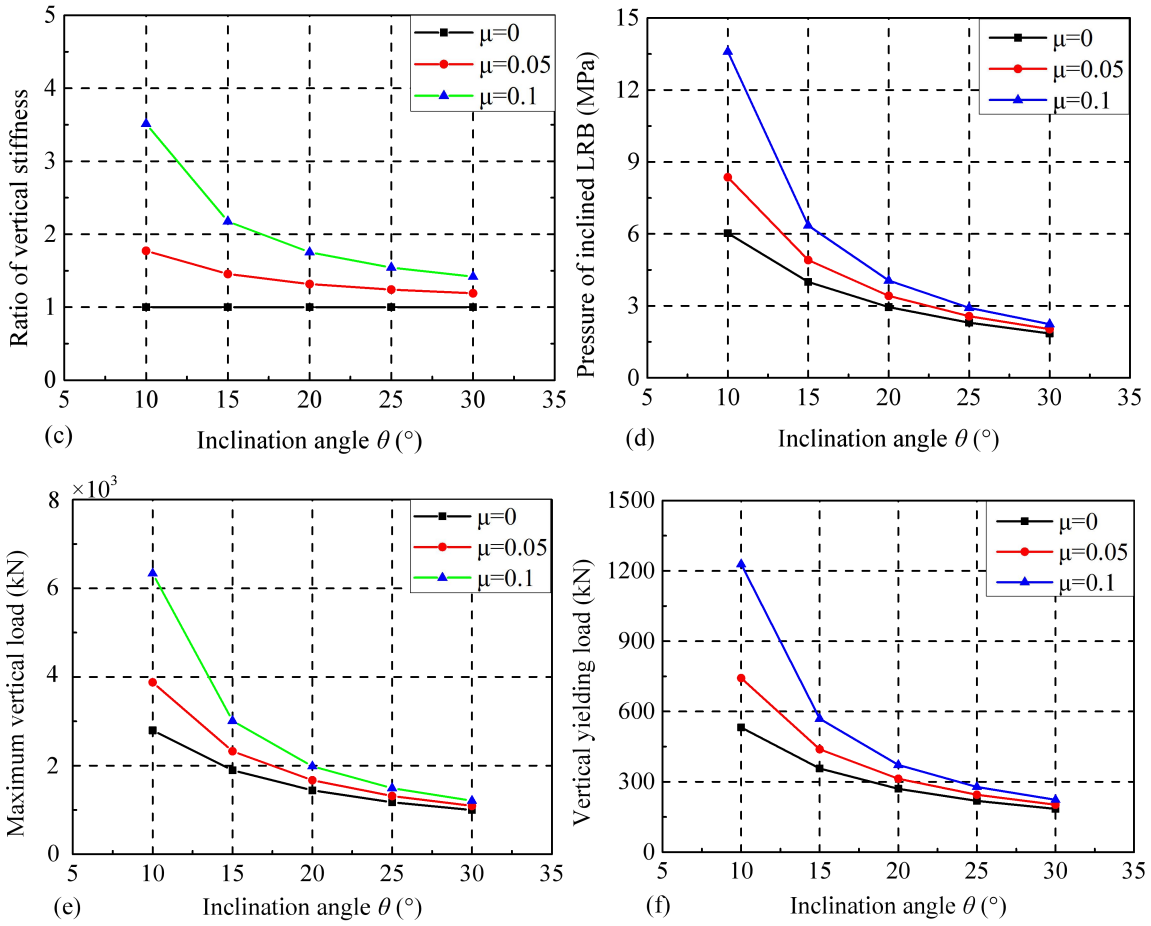

Fig. 8. Variation in the mechanical properties with inclination angle and friction coefficient: (a) variation in post-yield loading stiffness with inclination angle; (b) variation in post-yield unloading stiffness with inclination angle; (c) variation in loading and unloading stiffness ratio with inclination angle; (d) variation in LRB pressure with inclination angle when the shear strain is 100%; (e) variation in maximum vertical load with inclination angle; (f) variation in vertical yielding load with inclination angle.

The friction coefficient and inclination angle of the inclined LRBs strongly influence the vertical behavior of the proposed device. Fig. 8 (a and b) shows that the vertical stiffness of the 3D ORFSI decreases with increasing inclination angle. The vertical stiffness varies dramatically when the inclination angle is lower than 15° and slightly when the inclination angle is larger than 15°. The variation in the ratio of the vertical post-yield loading and unloading stiffness is shown in Fig. 8 (c). When the friction coefficient is 0, the loading and unloading stiffness remain the same, and the mechanical model degenerates into a conventional bilinear model. When friction exists, the loading stiffness is greater. The pressure of the inclined LRB when its shear strain is 100% is presented in Fig. 8(d). The pressure increases with the friction coefficient. The pressure decreases and the influence of the friction reduces with inceasing inclination angle. The highest pressure for inclination angles between 12° and 30° is lower than 10 Mpa. The variation in the maximum vertical load and vertical yielding load with inclination angle are displayed in Figs. 8 (e and f), respectively. The maximum vertical load is defined as the vertical load when the shear strain of the inclined LRB is 300%. The maximum vertical load and vertical yielding load decrease with increasing inclination angle and decreasing friction coefficient. The influence of the friction reduces with increasing inclination angle.

4. Conclusions

In this paper, a novel 3D ORFSI was proposed, and the static test was conducted. Based on test results, the asymmetric hysteretic model and parametric analysis of the 3D ORFSI system was studied. The main conclusions drawn from this study are as follows:

(1) In the proposed device rubber bearings are installed with inclination angle and it can transform vertical deformation into shear-torque-compression of the inclined bearings. Thus a balance between high supporting capacity and low vertical stiffness can be realized. The vertical hysteretic loop of the 3D ORFSI system is asymmetrically quadrilateral, and the stiffness in the loading process and unloading process are different.

(2) A vertical compression test of 3D isolator was conducted. The mechanical model of 3D ORFSI system was established, and the corresponding calculation formulas of the proposed model were presented. The proposed hysteretic model was then compared with the test result for validation, which shows good agreement (within 15% error). The proposed mechanical model is able to be used in simulating the vertical behavior of the proposed system with a reasonable accuracy.

(3) Parametric analyses were conducted. It is found that the inclination angle and friction have strong influence on vertical performance of 3D ORFSI system.

5. Acknowledgements

The research presented in this paper was supported by the National Natural Science Foundation of China (Nos. 51778355 and 51778356). The authors also want to acknowledge the Shanghai Nuclear Engineering Research & Design Institute Co., Ltd. for providing the ground motions used in this project.

6. References

[1] Staehlin WE, Chatham W, Hernandez A, Retamal E, Thiel CC, & Cluff L, et al (1996): Miscellaneous building types. *Earthquake Spectra, 12*(S1), 229–278.

[2] Gavin HP, & Nigbor RL (2012): Performance of the base-isolated christchurch women's hospital in the sep. 4, 2010 darfield earthquake and the Feb. 22, 2011 christchurch earthquake. *Proc., 20th Analysis and Computation Specialty Conf., ASCE Structures Congress,* ASCE, Reston, VA.

[3] Ryan KL, Soroushian S, Maragakis EM, Sato E, Sasaki T, & Okazaki T (2016). Seismic simulation of an integrated ceiling-partition wall-piping system at E-Defense. I: three-dimensional structural response and base isolation. *Journal of Structural Engineering, 142*(2), 04015130.

[4] Architectural Society of Japan. Liu W, Translation (2003): *Recommendation for the design of base isolated buildings,* Seismological Press, Beijing, China (in Chinese).

[5] Yang J, & Lee CM (2007): Characteristics of vertical and horizontal ground motions recorded during the Niigata-ken Chuetsu, Japan Earthquake of 23 October 2004. *Engineering geology*, 94(1-2), 50-64.

[6] Fujita S, Kato E, Kashiwazaki A, Shimoda IK, & Sasaki KO (1996): Shake table tests on three-dimensional vibration isolation system com-prising rubber bearing and oil spring. *In Proc., 11th World Conf. on Earthquake Engineering*. Acapulco, Mexico: Mexico Society of Seismic Engineers.

[7] Garevski M, Kelly JM, & Zisi N (2000): Analysis of 3D vibrations of the base isolated school building "Pestalozzi" by analytical and experimental approach. *Proceedings of the 12th WCEE*, Auckland, New Zealand.

[8] Ogiso S, Nakamura K, Suzuki M, & Moro S (2003): Development of 3D seismic isolator using metallic bellows. *In Proc., Transactions of the 17th Int. Conf. on Structural Mechanics in Reactor Technology (SMiRT 17).* Prague, Czech Republic: State Office for Nuclear Safety of the Czech Republic.

[9] Morishita M, Kitamura S, Moro S, & Fushimi M (2003): Development of 3D seismic isolation technology for advanced nuclear power plant application.

[10] Inoue, K., Morishita, M., & Fujita, T (2004, January): Development of three-dimensional seismic isolation technology for next generation nuclear power plant in Japan. In *ASME/JSME 2004 Pressure Vessels and Piping Conference* (pp. 29-34). American Society of Mechanical Engineers Digital Collection.

[11] Ueda M, Ohmata K, Yamagishi R, & Yokoo J (2007): Vertical and three-dimensional seismic isolation tables with bilinear spring force characteristics: for which a Λ-shaped link mechanism is used. *Transactions of the Japan Society of Mechanical Engineers, Series C, 73*(735), 2932-2939.

[12] Tomizawa T, Takahashi O, Aida H, Suhara J, Saruta M, Okada K, ... & Fujita T (2013, January): Vibration test in a building named 'Chisuikan'using three-dimensional seismic isolation system. *In 15th International structural engineering and construction conference* (pp. 791-796).

[13] Liu W, & Imam M (2013): The earthquake response analysis of base isolated structures using a new 3d seismic isolator. Shanghai: Shanghai University.

[14] Vu B, Unal M, Warn GP, & Memari AM (2014): A distributed flexibility and damping strategy to control vertical accelerations in base-isolated buildings. *Structural Control and Health Monitoring, 21*(4), 503-521.

[15] Zhou Z, Wong J, & Mahin S (2016): Potentiality of using vertical and three-dimensional isolation systems in nuclear structures. *Nuclear Engineering and Technology, 48*(5), 1237-1251.

[16] Jia JF, Dong HH, Zhang T, & Du XL (2014): Mechanics performance test and seismic behavior of a novel 3D isolation bearing for bridges. *In International efforts in lifeline earthquake engineering* (pp. 441-448).

[17] Eltahawy W (2017, January): Fundamental dynamics of 3-dimensional seismic isolation. *In 16th World Conference on Earthquake Engineering*.

[18] Liu W, Xu H, He W, & Yang, Q (2018): Static test and seismic dynamic response of an innovative 3D seismic isolation system. *Journal of Structural Engineering*, 144(12), 04018212.

